

A Study of Channel Optimization in Cooling Spreader on a Smaller and Transient Heat Source

K. Yazawa* and M. Ishizuka**

*Sony Corporation, Shinagawa, Tokyo, Japan; Kazuaki.Yazawa@jp.sony.com

**Toyama Prefectural University, Imizu, Toyama, Japan

ABSTRACT

Due to the continuous growth of the performance of micro processors, further extension of heat removal performance from the chip to the ambient is needed. As one of the corresponding research, micro-channel cooling with integrated into a die has been precisely and extensively studied. Although, slightly larger cooling channels with spreading form small area, namely a miniature channel, is desired in some cases of realistic design since there is a limitation of pumping power by system packaging requirement. Since the spreader section is assumed in the miniature channel it should be designed properly to spread the heat from smaller area to the entire channel area, the trade off between spreading and convection performance of the channel is investigated. The model proposed in combination of thermofluidic model and spreading conduction model was investigated and validated with numerical calculation. This model is found consist to the numerical results within less than 10% except a case of high flow rate condition, which will hardly exists in consumer electronics. Further more, the step input transient response of heat source temperature is also investigated and found appropriate to be utilized in design. Through the parametric study based on static model, it can be concluded that the deeper channel with small outline with thicker base is the best profile for the miniature channel coolers while only small pumping power is available

NOMENCLATURE

A	Area [m ²]
B	Thickness of base section of channels [m]
c	Specific heat [J/kg K]
C	Thermal capacitance [J/K]
D_h	Hydraulic diameter [m]
h	Heat transfer coefficient [W/m ² K]

H	Channel height (depth) [m]
k	Thermal conductivity [W/mK]
K	Contraction and expansion coefficient
L	Length of channel [m]
P	Pressure [Pa]
Q	Heat generation [W]
t	Time, elapsed time [sec]
T	Temperature [C]
u	Velocity [m/sec]
V	Volumetric flow rate [m ³ /sec]
w	Gap of channel [m]
W_{pp}	Pumping power [W]

Greek symbols

α	Thermal diffusivity [m ² /sec]
β	Geometry factor [1/m]
ρ	Density [kg/m ³]
σ	Contraction ratio
Ψ	Thermal Resistance [K/W]

Subscripts

a	Ambient
B	Base plate for spreading
E	External boundary
F	Channel section
P	Plate for 1-D conduction
S	Spreading

INTRODUCTION

Corresponding to the growth of power in processors as ITRS has been indicating (2004), micro channel cooling on high performance processors has been studied quite well since Tuckerman (1981). A single phase and simple parallel

channels micro channel cooling for up to 100 W/cm^2 is promising at least at the test bed in the laboratory. However, it has been hard to implement it in a trendy compact/slim design computers or consumer electronics. The most of the difficulties are originated from the high pressure head required to pump the coolant fluid through the channels. Singhal et al. (2004) and Garimella et al. (2003) reviewed the pressure impact on a various type of micro channels. The objective of this study is to understand the performance of the miniature channel cooler which allows the efficient use of the pump with significantly lower pumping power as well as to establish a model for the design.

The channel gap in the miniature cooler is in range of 100 microns to 1mm wide and various height aspect ratios from 1 to 8. Since the channels are one order larger than a well characterized channel (e.g. Judy et al. (2002) done), the profile of the cooler becomes larger than the heat source, which is typically assumed $1.0 \times 1.0 \text{ cm}$ silicon chip. To build and attach the cooler with minimum spreading resistance, it is necessary to optimize the dimensions with proper range of volumetric flow rate of pumped coolant. In an oversized block, the channels are grooved on the properly thicker base section where the heat source attached. There was an optimization work on micro channels as Knight et al. (1992), but there was not found the references which studied or modeled the performance of micro channels with such spreading combination. Thus an analytic model is proposed and verified with the numerical calculation. In the process, we found interesting back effect to the spreading by the liquid flow through the channel. This characteristic is discussed and modeled. This validated model allows the optimization work on various geometry studies. And we will discuss the transient thermal resistance at the source temperature view point. The transient spreading model is based on our previous work Yazawa et al. (2005).

MODEL

The miniature cooler is a block which has the square foot print in this case with proper thickness attached on the square and uniformly heated source. All channels in a block are made same width and depth in parallel each other. The well thickness (Line) and gap (Space), so called “L/S”, are set to unity for all channels. Inlet and outlet of the channels are assumed uniform flow in a duct with same height of channels. For the numerical calculation, 100W of heat is applied on $1.0 \times 1.0 \text{ cm}$ area place at the exact center of the miniature cooler. The coolant fluid is water at 40°C , 1atm condition. The cooler block is made of pure copper. The miniature channel geometry is shown in Fig.1~3. Some of the concept of developing fluiddynamic modeling and heat transfer modeling is following Yazawa et al. (2003).

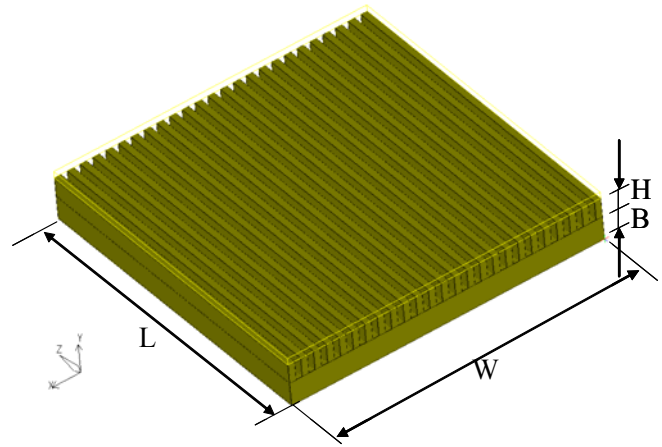


Fig. 1 Miniature channel geometry

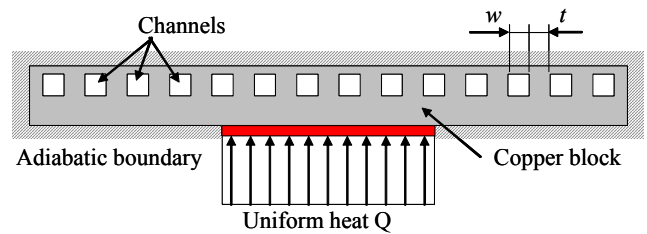


Fig. 2 Cross section of the model of heat sink base

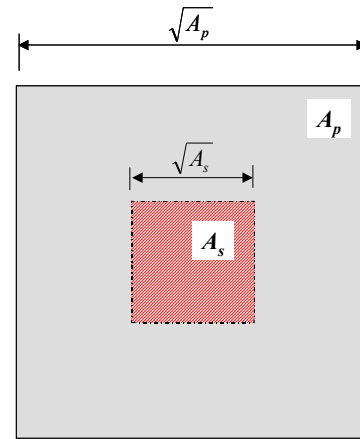


Fig. 3 Plane view of the base plate; the heat source area in the middle

Definition of overall thermal resistance is as Eq. (1).

$$\Psi = \Psi_s + \Psi_f = \frac{(T_{\max} - T_a)}{Q} \quad (1)$$

where, subscripts s of thermal resistance denotes the spreading contribution of the base section and f indicates the heat transfer contribution of channels, respectively. Supplied power W_{pp} to generate the airflow is defined as Eq. (2).

$$W_{pp} = \dot{V}\Delta P \quad (2)$$

Fluid Dynamic Modeling

Mean velocity u in a channel can be defined with volumetric mean velocity V driven by a pump as Eq.(3).

$$u = \frac{Nw}{W}V \quad (3)$$

where, mean velocity in duct V comes from whole volumetric flow rate V as Eq. (4).

$$V = \frac{\dot{V}}{(WH)} \quad (4)$$

Fluid dynamics of rectangular channels are modeled by using similarity on circular channel. D_h is channel based hydraulic diameter defined with cross section area of the channel divided by wetted perimeter as Eq. (5).

$$D_h \equiv \frac{4 \times Area}{Perimeter} = \frac{2Hw}{(H+w)} \quad (5)$$

The wall friction loss due to the fluid viscosity at the near wall causes the pressure loss. A laminar flow is assumed and developing flow at the entrance region is considered. The pressure difference from the entrance to exit is formulated as Eq. (6).

$$\Delta P = \frac{K\rho}{2}u^2 + \Delta P_{wall} \quad (6)$$

Contraction loss coefficient K_c and expansion loss coefficient K_e are considered for the channel flow pressure loss according to Kays and London (1984).

$$K = (1 - \sigma_c^2 + K_c) - (1 - \sigma_e^2 - K_e) \quad (7)$$

Clearly, $\sigma_c = \sigma_e = \sigma$ since the entrance and the exit geometry is exactly flip as Fig. 4.

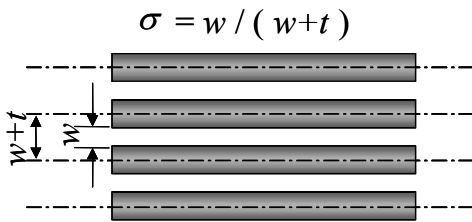


Fig. 4 Flow entrance and exit

The wall pressure loss as the second part of Eq. (6) is found as Eq. (8). The apparent friction coefficient for a

various aspect ratio rectangular channels is found as Eq. (9) according to the plot of Kays and Crawford (1993) in fully developed flow. The approximate function is modified from circular tube to the rectangular channel by multiplying by 24/16. The fully developed profile is found at $Re / (L / D_h) = 20$ or for larger L . Developing flow yields flow resistance to be greater than fully developed flow. Developing friction factor is defined with approximate function as Eq. (10) according to Langhaar's plot (1942) as a single apparent mean friction coefficient ratio y , whose formulas are separately defined based on entry length.

$$\Delta P_{wall} = 2C_{app} \frac{\rho u^2 L}{D_h} \quad (8)$$

$$C_{app} = \frac{24}{Re} y (1 - 1.3553\alpha + 1.946\alpha^2 - 1.7012\alpha^3 + 0.9564\alpha^4 - 0.2537\alpha^5) \quad (9)$$

where,

$$y = \frac{24}{16} \left\{ 0.202 \frac{Re}{L/D_h} + 16 \right\}, \quad \left(\frac{Re}{L/D_h} < 20 \right) \quad (10)$$

$$y = \frac{24}{16} \left\{ 6.128 \left(\frac{Re}{L/D_h} \right)^{0.3915} \right\}, \quad \left(\frac{Re}{L/D_h} \geq 20 \right)$$

while, Reynolds number Re is defined by Eq.(11).

$$Re = \frac{\rho u D_h}{\mu} \quad (11)$$

Channel Heat Transfer

Assuming isothermal channel wall surface, as well known, deferential energy balance equation yields,

$$\frac{T_s - T_m}{T_s - T_i} = \exp\left(-\frac{hS}{\rho C_p \dot{V}}\right) \quad (12)$$

where, T_s : wall surface temperature, T_i : Inlet air temperature and T_m : Log mean air temperature over the entire channel length, h : mean heat transfer coefficient on channel and S : heat transfer surface area is found by Eq. (13).

$$S = 2(w + H)L \quad (13)$$

Thermal resistance of sensible temperature rise of air in the channel can be expressed as Eq. (14).

$$\Psi_{cap} = \frac{1}{N\rho C_p \dot{V}} = \frac{1}{N\rho C_p HwV} \quad (14)$$

Accordingly, total thermal resistance Ψ_f for convection part can be formulated as Eq. (15).

$$\Psi_f = \Psi_{cap} \frac{1}{(1 - \exp(-hS\Psi_{cap}))} \quad (15)$$

In the channel, the wall temperature is assumed uniform since the height/width ratio of fin is limited to 8 and the fin is made of high thermal conductive material. Therefore, fin efficiency will not be significantly necessary.

Channel based Nusselt number Nu is related to the rectangular channel cross-section geometry for fully developed laminar flow and isothermal walls, is found as,

$$\Psi_{conv} = \frac{1}{hS} \quad (16)$$

where, h : is heat transfer coefficient based on the channel Nusselt number and the previous definition of hydraulic diameter as Eq. (17).

$$h = \frac{Nuk_f}{D_h} \quad (17)$$

The Nusselt number here must be fully compatible to various aspect ratios and a various length of the channels. Since the four channel walls are made of same solid material, the channel can be modeled as four wall heated. To find the approximate function to predict the channel heat transfer, following model is proposed as Eq. (18).

$$Nu = \frac{Nu_m(x^+)}{2.98} Nu_H \quad (18)$$

where, x^+ is defined as Eq. (19) and the dimension less entry length is found at $x^+ = 0.1$. L^+ is the thermal entry length.

$$x^+ = \frac{2(L^+ / D_h)}{\text{Re Pr}} \quad (19)$$

Based on Kays and Crawford (1993), mean Nusselt number Nu_m over the entire length of the channel from the entry is introduced. The following formula is a series-solution for a square tube.

$$Nu_m = \frac{1}{2x^+} \ln \left[\frac{1}{8 \sum_{n=0}^{\infty} (G_n / \lambda_n^2) \exp(-\lambda_n^2 x^+)} \right] \quad (20)$$

where, G_n and λ_n values available from $n = 0$ to 2 in table 1 are sufficiently significant for $x^+ > 0.01$.

N	λ_n^2	G_n
0	5.96	0.598
1	35.64	0.462
2	78.9	0.138

Table 1

Since x^+ converges while $L \rightarrow \infty$, the number 2.98 in Eq. (18) which is equal to $Nu_m(\infty)$ represents the heat transfer at the fully developed thermal boundary.

For the aspect ratio correlation with assuming laminar and fully developed thermal boundary on the uniformly heated wall, following approximation function can be formulated according to the data points in Shah and London (1978).

$$Nu_H = 8.235 (1 - 2.0421\alpha + 3.0853\alpha^2 - 2.4765\alpha^3 + 1.0578\alpha^4 - 0.1861\alpha^5) \quad (21)$$

where, α : channel aspect ratio.

$$\alpha = \frac{H}{w} \quad (22)$$

Spreading Thermal Resistance

The model has the spreading section beneath the channels. Spreading thermal resistance from a square heat source to a square solid block with the effective heat transfer coefficient, which represents the channel heat transfer, on top of the block and rest of adiabatic boundaries is already modeled by Lee et al. (1995) very accurately as Eq. (23).

$$\psi_S = \frac{\sqrt{A_P} - \sqrt{A_S}}{k_B \sqrt{\pi A_P A_S}} \frac{\beta k_B A_P \psi_f + \tanh(\beta B)}{1 + \beta k_B A_P \psi_f \tanh(\beta B)} \quad (23)$$

where B is the plate thickness, k_B the thermal conductivity of the plate, and β the geometry factor is

$$\beta = \frac{\pi^{1.5}}{\sqrt{A_P}} + \frac{1}{\sqrt{A_S}} \quad (24)$$

In this channel, B_{eff} : effective thickness encountered for spreading is base plate thickness plus the copper ratio of channel section. It becomes as Eq. (25).

$$B_{eff} = B + \frac{Nw}{W} H \quad (25)$$

In the miniature channel, the sensitive temperature rise of airflow is assumed to effect back to the spreading in the block. The effect of flow passage is encountered as follows.

$$k_{S_eff} = \frac{1}{2\psi_{cap}} \left(\frac{L-L^+}{L} \right)^2 \quad (26)$$

where, L^+ is thermal entry length.

Transient Temperature Rise at Heat Source

Following Yazawa et al (2005), the transient spreading has been modeled based on dimensionless time function of half space spreading model by Yovanovich (1997) as Eq. (27).

$$\begin{aligned} \psi(t) = & (\psi_B + \psi_E) \left(1 - \exp\left(\frac{-t}{C_B(\psi_B + \psi_E)}\right) \right) \\ & + \psi_S \left\{ 2 \sqrt{\frac{k_B}{\rho c A_S}} t \left(1 - \exp\left(\frac{-\rho c A_S}{4\pi k_B t}\right) \right) \right\} + \psi_S \left\{ \operatorname{erfc}\left(\frac{1}{2} \sqrt{\frac{\rho c A_S}{\pi k_B t}}\right) \right\} \end{aligned} \quad (27)$$

where,

$$\psi_E = \frac{1}{hA_p} \quad (28)$$

$$\psi_B = \frac{L}{\lambda A_p} \quad (29)$$

and,

$$C_B = C_P = \rho_B c_B A_p L \quad (30)$$

NUMERICAL MODELING

The model previously established was compared with the numerical analysis. Thermo-fluid analysis software ICEPAK was used for the simulations. The channel and base block were modeled with copper material property and the fluid represents the material property of water at 40°C. In addition to the channel section the entrance and exhaust duct was modeled for 5mm length and with the exact same height as the channel. The mesh was approximately 250,000 ~ 400,000 depend on the geometry. Velocity, pressure and temperature were calculated in double precision with second order discretization to prevent the linear prediction errors. The convergence criteria of residue were set to 1e-3 for momentum and 1e-7 for energy equation in all calculations.

COMPARISONS AND DISCUSSIONS

As shown in the Fig. 5~7, the analytically predicted pressure loss through the channel consists to the numerical calculation over the various geometries and flow rates. These three of the models are designed for constant volume of the miniature cooler $2e-6 \text{ m}^3$ and the volumetric flow rate is fixed at $1.67e-5 \text{ m}^3/\text{sec}$. The results are reasonably in agreement with over all error of thermal resistance was found less than 10%.

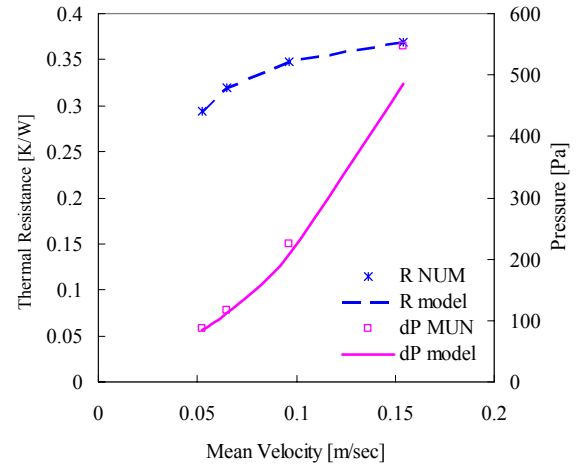


Fig. 5 Thermal resistance and pressure by mean velocity
L=0.0205, H+B=4.76mm

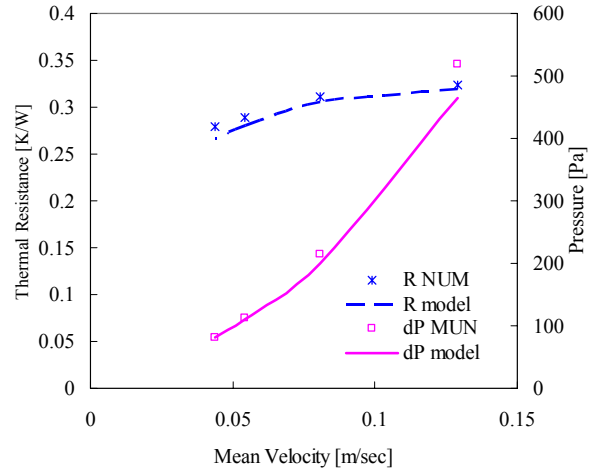


Fig. 6 Thermal resistance and pressure by mean velocity
L=0.0245, B+H=3.33mm

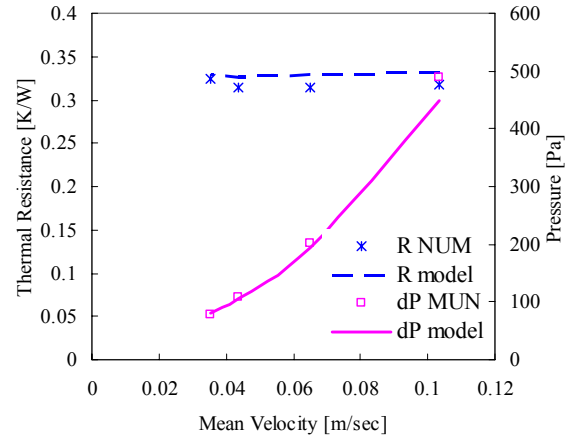


Fig. 7 Thermal resistance and pressure by mean velocity
L=0.0305, B+H=2.15mm

The following figure shows the thermal performance and pressure loss depending on the volumetric flow rate on the same geometry as Fig 6 configuration.

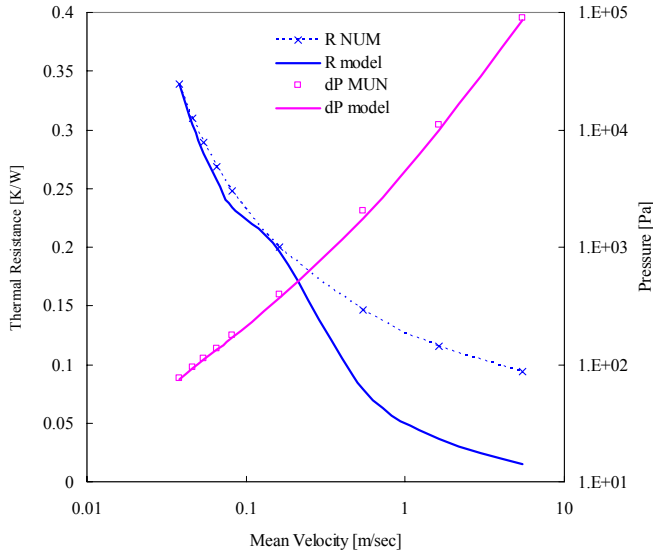


Fig. 8 Thermal resistance and Pressure for wide range flow rate

There found great agreement in pressure drop over the wide range of flow rate. It should be noted that the numerical calculation is done by laminar solver. Thus, it is meaningless if the flow regime is turbulent. Thus, we should carefully check the Reynolds number while we see the results. In this case, $Re=2000$ is found at around 0.8m/sec of mean velocity at the case of Fig.8.

If the thermal entrance length is smaller than the half length of the base length, analytically predicted thermal resistance consists well. However, the entry length exceed the limit, the prediction fails.

Figure 9 shows the detailed temperature profile across the channel. Open mark represents the base temperature and solid mark represents the fluid temperature at center of flow. The base temperature profile can be seen reasonable while spreading and convection is mixed.

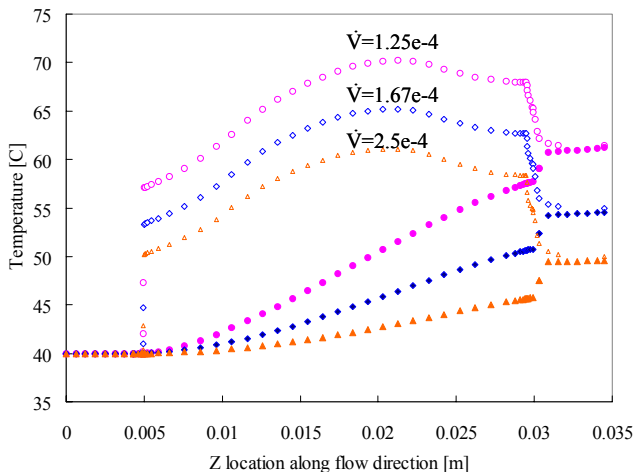


Fig.9 Temperature profile along the channel length

Cooling performance, which is an inverse of thermal resistance, is better as pumping power is larger in overall as Figure 10 shows. It can be noted that the optimum channel height varies based on flow rate and channel geometry. For the case-A, there is an optimum and the larger height is better for case-B. The larger height of channel allows larger flow rate in same outline of the miniature channel. As seen in the same figure, the impact of base thickness is also significant for total thermal resistance. The appropriate thickness for $L=24.5$ / $A=10.0\text{mm}$ spreading at around 7.7mm for case-A and 7.7mm for case-B while 5% over the optimum thermal resistance is allowed, respectively.

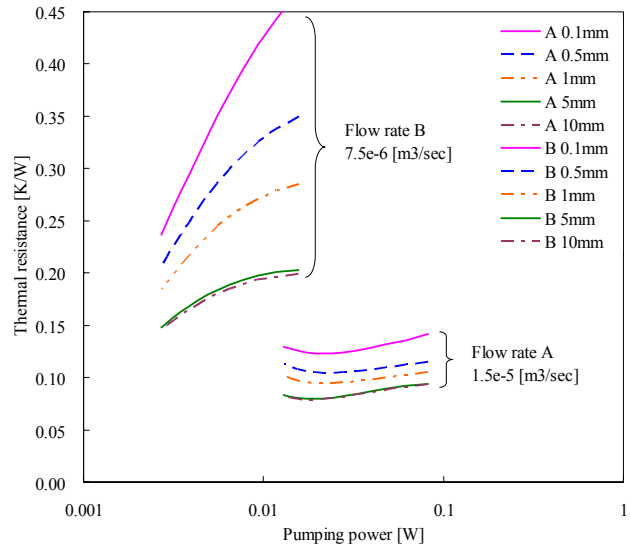


Fig. 10 Thermal performance by pumping power for the study cases

Fig 11 shows the geometry optimization study result sorted by pumping power. Studied ranges are $0.001 < B < 0.005$, $6e-4 < H < 1.8e-3$ and $0.02 < L < 0.04$. As number of channels, the performance is improving generally. Near optimum geometry, it is noted that the channel aspect is large as much as possible and size of the bock is the smallest for the studied cases. The broken line curves in the figure represent the region where thermal entry length is too large to find correct solution. The best solution in this study was found at $W_{pp}=0.03\text{W}$ and geometry of 20mm case, 1.8mm depth and 0.225mm space 45 channels with 5mm thick base. This configuration is predicted 0.0586K/W thermal resistance at 10mm heat source.

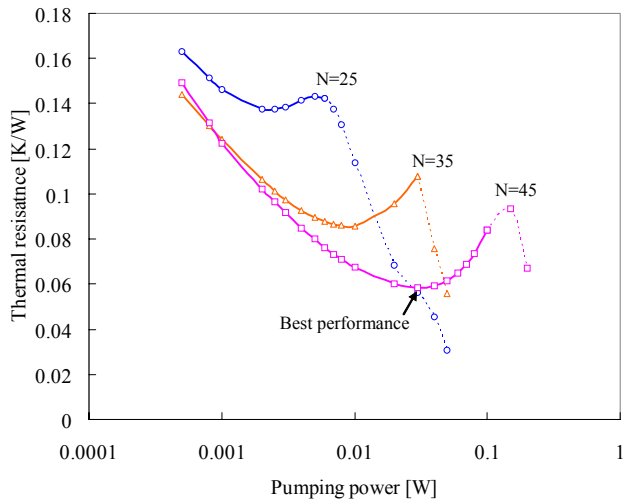


Fig. 11 Thermal resistance resulting from the geometry optimization study

Figure 12 shows the transient thermal resistance of source to ambient compared with numerical analysis while the step heat input applied at $t=0$ as the flow is stable over the time. The absolute error of steady state on thermal resistance was found 0.97% for the case. The model consists well over the time so that our approach of transient analysis is applicable to these miniature channels.

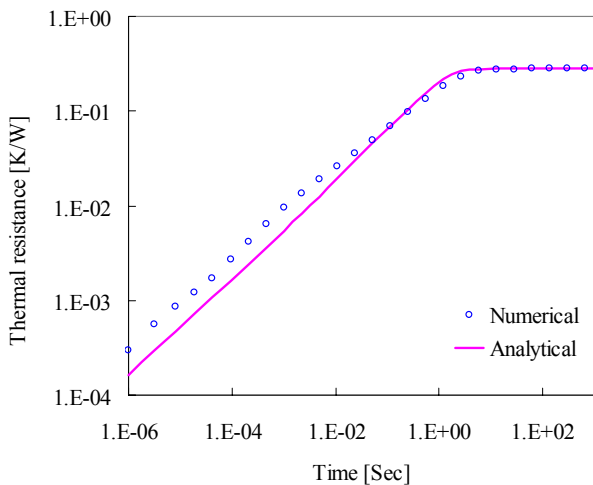


Fig. 12 Transient thermal resistance response to step function of heat input at $t=0$
 $L=0.0245$, $H=0.0012$, $B=0.00213$

Following three figures shows the cross section temperature map in the results of numerical calculations. At the early stage of heating. The film thermal conduction is observed very near region above the heat source. Interestingly, the temperature propagates almost uniformly regardless to the flow direction at the early propagating stage. As entire channel approaching steady state, the temperature profile is influenced by flow direction as seen in Fig. 15. Also, the temperature rise of fluid in passage is observed.

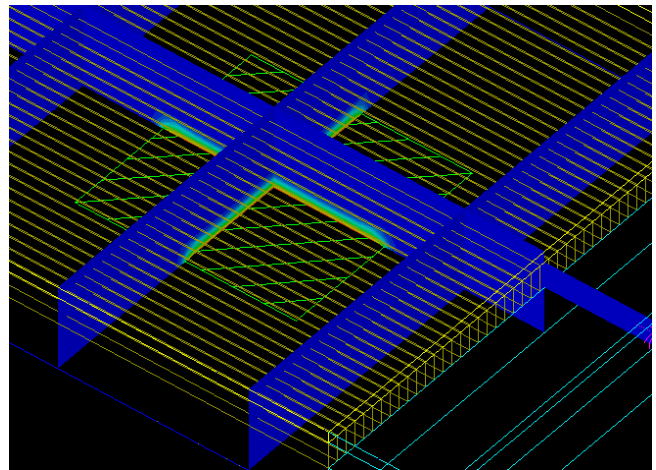


Fig. 13 Temperature map at $t=0.001\text{sec}$

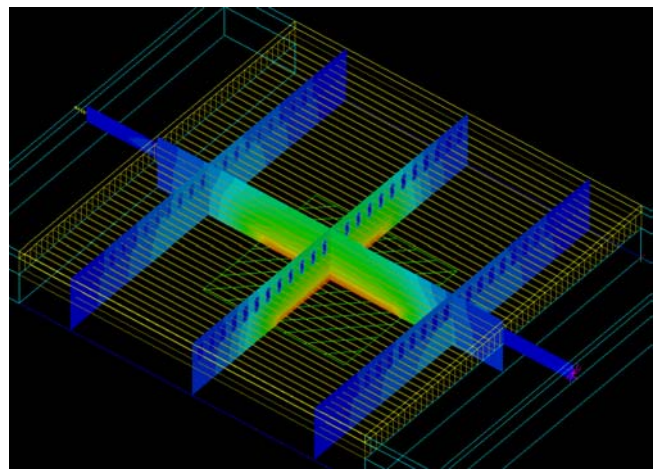


Fig. 14 Temperature map at $t=0.1\text{sec}$

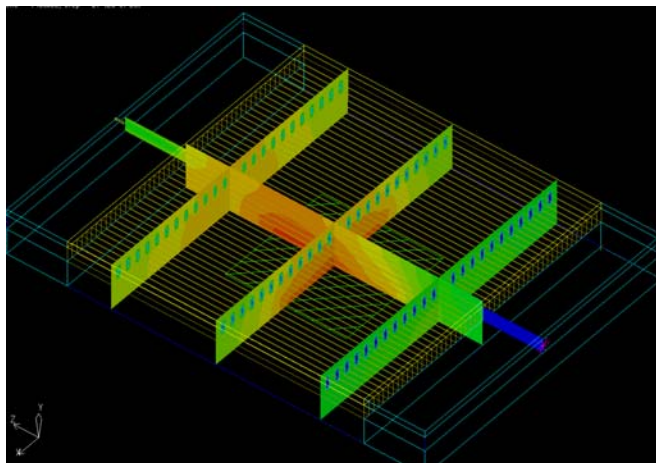


Fig. 15 Temperature map at $t=1000\text{sec}$

CONCLUSIONS

The miniature channel is modeled by superimposing the spreading with channel flow dynamic and heat transfer models and tested with numerical simulation in steady state and step input transient response. The models shows good agreement with less than 10% error in range of the relatively slow flow and the limitation of this model is exist at the thermal entry length exceed the half way of the channel length. As well as transient response successfully agreed with the numerical model.

From the extensive parametric analysis, the thicker base section is better for the performance in general. The pressure head required to the pump is significantly reduced by enlarge the channel dimension with our significant change of thermal resistance. To maintain the smaller spreading thermal resistance, the larger channel aspect ratio is the better. The best cooling performance over the studied case was found 0.0586K/W for the 0.03W pumping power. These results are greatly helpful for the low cost design of consumer electronics with utilizing these miniature channels.

REFERENCES

- SIA, 2004, *International Technology Roadmap for Semiconductors 2004 update of 2003 SIA road map*
- Tuckerman, D. B. and Pease, R. F. W., 1981, High-performance heat sinking for VLSI, *IEEE Electron Device Letters*, Vol. 2, pp. 126-129
- Singhal, V., Garimella, S.V. and Raman A., 2004, Microscale pumping technologies for microchannel cooling systems, *Applied Mechanics Review* Vol. 57, No. 3.
- Garimella S.V. and Sobhan C.B., 2003, "Transport in microchannels—A critical review", *Annu. Rev. Heat Transfer*, Vol. 15
- Judy, J., Maynes, D. and Webb, B. W., 2002, Characterization of frictional pressure drop for liquid flows through microchannels, *Int. J. Heat Mass Transfer*, Vol. 45, pp. 3477- 3489.
- Knight, R. W. et al, 1992, Heat Sink Optimization with Application to Microchannels, *IEEE Transaction on Components, Hybrids and Manufacturing Technology*, Vol. 15, No. 5
- Yazawa, K. and Ishizuka, M, 2005, Thermal Modeling with Transfer Function for the Transient Chip-On-Substrate Problem, *Thermal Science & Engineering*, Vol. 13, No. 1, p. 37
- Yazawa K., Solbrekken, G. L. and Bar-Cohen, A., 2003, Thermofluid Design of Energy Efficient and Compact Heat Sink, *Proceedings of InterPACK, IPACK 2003-35242*
- Kays, W. M. and London, A. L., 1984, *Compact Heat Exchangers*, McGraw-Hill, New York, NY.
- Kays, W. M. and Crawford, M. E., 1993, *Convective Heat and Mass Transfer*, Third Edition, McGraw-Hill, New York.
- Langhaar, H. L., 1942, *Applied Mechanics*, Vol. 9
- Shah, R.K., and London, A. L., 1978, *Laminar Flow Forced Convection in Ducts*, Supplement 1 to Advances in Heat Transfer, Academic Press, New York.
- Lee, S. et al, 1995, Constriction/Spreading Resistance Model for Electronics Packaging, *Proceedings of ASME/JSME Thermal Engineers Conference*, pp199-206
- Yovanovich, M., 1997, Transient Spreading Resistance of Arbitrary Isoflux Contact Areas: Development of a Universal Time Function, *Proceedings of the 32nd Thermophysics Conference*, AIAA.